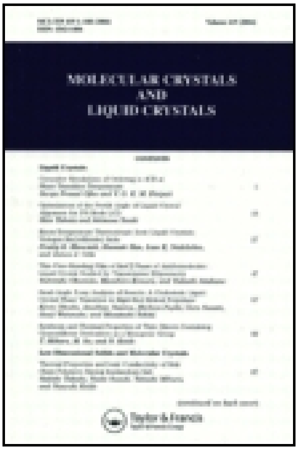

Molecular Crystals and Liquid Crystals
Publication details, including instructions for authors and subscription information:
http://www.tandfonline.com/loi/gmcl20

Fragility and Glass Transition Temperature in the Rheological Response of Azobenzene Copolymers

L. Andreozzi [a], M. Faetti [a], M. Giordano [a], F. Zulli [a], G. Galli [b] & S. Samaritani [b]

[a] Dipartimento di Fisica "E. Fermi" and polyLab INFM, Università di Pisa, Italy

[b] Dipartimento di Chimica e Chimica Industriale and INSTM, Università di Pisa, Italy

To cite this article: L. Andreozzi, M. Faetti, M. Giordano, F. Zulli, G. Galli & S. Samaritani (2006): Fragility and Glass Transition Temperature in the Rheological Response of Azobenzene Copolymers, Molecular Crystals and Liquid Crystals, 450:1, 173/[373]-182/[382]

To link to this article: http://dx.doi.org/10.1080/15421400600588132

Mol. Cryst. Liq. Cryst., Vol. 450, pp. 173/[373]–182/[382], 2006
Copyright © Taylor & Francis Group, LLC
ISSN: 1542-1406 print/1563-5287 online
DOI: 10.1080/15421400600588132

Fragility and Glass Transition Temperature in the Rheological Response of Azobenzene Copolymers

L. Andreozzi
M. Faetti
M. Giordano
F. Zulli
Dipartimento di Fisica "E. Fermi" and polyLab INFM,
Università di Pisa, Italy

G. Galli
S. Samaritani
Dipartimento di Chimica e Chimica Industriale and INSTM,
Università di Pisa, Italy

Two copolymers containing nonmesogenic methyl methacrylate (MMA) and nematogenic azobenzene methacrylate (MA4) side groups (30/70 and 40/60 copolymers) azobenzene were studied in the linear viscoelastic regime. The time-temperature superposition principle was found to hold over the whole investigated temperature range, even across the nematic-isotropic transition in the 30/70 copolymer. Rheological steady state and oscillatory measurements were used to obtain the temperature dependence of the zero shear viscosity. The strength and dynamic fragility of these two copolymers were compared with those of the corresponding PMA4 and PMMA homopolymers, which pointed out the role of the structure of the main chain in dictating the relaxational dynamics.

Keywords: azobenzene; liquid crystal polymer; nematic; rheology; shear viscosity

INTRODUCTION

In the last years, side group liquid crystalline polymers have proved to be suitable candidates as media for optical information storage, especially those containing photoresponsive azobenzene side groups [1]. We recently accomplished in fact optical writing at both micrometer

Address correspondence to L. Andreozzi, Dipartimento di Fisica "E. Fermi" and polyLab INFM, Università di Pisa 56127, Pisa, Italy. E-mail: laura.andreozzi@df.unipi.it

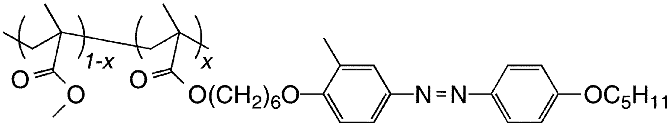

FIGURE 1 Structure of PMA4 homopolymer ($x = 1$), 30/70 ($x = 0.7$) and 40/60 ($x = 0.6$) copolymers, and PMMA homopolymer ($x = 0$).

and nanometer length scales in the nematic polymethacrylate PMA4 system, either homopolymers or copolymers with methyl methacrylate (MMA), that consists of a spaced azobenzene side group as the nematogenic photoresponsive unit (Fig. 1) [2–4].

Achieving an effective, high-resolution and long-term data storage deals with crucial parameters such as bit stability, homogeneity at molecular level, and working temperature [2,3]. Therefore, a full characterization of the polymeric matrix should employ different spectroscopic techniques that can cover several length and time scales. Accordingly, we used electron spin resonance (ESR) spectroscopy to study the stability of different molecular sites and their correlation times as a function of temperature in PMA4 homopolymers and copolymers [2]. On the other hand, rheological measurements also evidenced the linear viscoelastic behavior of the PMA4 polymers, and the occurrence of a peculiar conformational transition in PMA4 homopolymers [2,5].

In the present work, we performed steady state and oscillatory measurements at different temperatures on PMA4 40/60 and PMA4 30/70 copolymers (Fig. 1), and found that the time-temperature superposition (TTS) principle holds over the whole investigated temperature range. The temperature dependence of the zero shear viscosity of the copolymers was also worked out and related to their strength and dynamic fragility in a comparison with those of the respective PMA4 and PMMA homopolymers.

MATERIALS AND EXPERIMENTAL

The PMA4 40/60 ($x = 0.60$) and 30/70 ($x = 0.70$) copolymers were prepared by free-radical polymerization [6]. The average molar masses and their distributions were determined by size exclusion chromatography with polystyrene standards (Table 1). Differential scanning calorimetry (DSC) measurements were performed with a Perkin-Elmer DSC7 calorimeter (10 K/min heating rate) frequently calibrated with indium and zinc standards. The glass transition temperatures T_g, and the nematic-isotropic temperatures T_{NI} are reported in Table 1.

TABLE 1 Physico-Chemical Characteristics of the PMA4 Copolymer Samples. Legenda: nd: not Resolvable from T_g

Copolymer	x	M_w (Da)	M_w/M_n	T_g (K)	T_{NI} (K)
PMA4 30/70	0.70	117000	3.54	314	345
PMA4 40/60	0.60	93200	4.01	320	nd

Rheological measurements, in both continuous and oscillatory regimes, were carried out with a Haake RheoStress RS150H rheometer in the plane-plate geometry (20 mm diameter) with varying temperature under highly pure nitrogen flow. In order to account for thermal dilatation of the system, the gap in the plane parallel geometry was automatically varied in the temperature range between 0.40 mm and 0.60 mm. The gap was chosen to ensure gap independent measurements. A TC501 thermo-controller unit kept the temperature of the sample stable within 0.1 K. Preliminary tests were conducted to ensure that all measurements were carried out in the linear viscoelastic regime.

RESULTS AND DISCUSSION

The rheological measurements were performed in the temperature ranges of 323–394 K and 335–438 K for the 30/70 and the 40/60 copolymers, respectively. The values of the zero shear viscosity were evaluated in independent ways with steady state flow and creep measurements and oscillatory measurements. In this case loss modulus G'' and viscosity η are related according to $\eta = \lim_{\omega\to 0}(G''/\omega)$. The viscosity data for PMA4 30/70 and PMA4 40/60 are shown vs. $1000/T$ in Figure 2. No discontinuity of the viscosity was observed in either sample, not even for the 30/70 copolymer at T_{NI}. The viscosity data were fitted with a Vogel-Fulcher law (VF):

$$\eta = \eta_\infty \exp\left(\frac{T_b}{T - T_0}\right) \tag{1}$$

The values of the pseudo-activation energy T_b, the Vogel temperature T_0, and η_∞ are given in Table 2.

The copolymers showed superimposable data of the storage G' and loss G'' moduli to reconstruct the master curve, even for the 30/70 copolymer with data recorded at temperatures below and above the nematic-isotropic transition (Fig. 3). This finding and the fact that viscosity data from oscillatory and steady state measurements were well

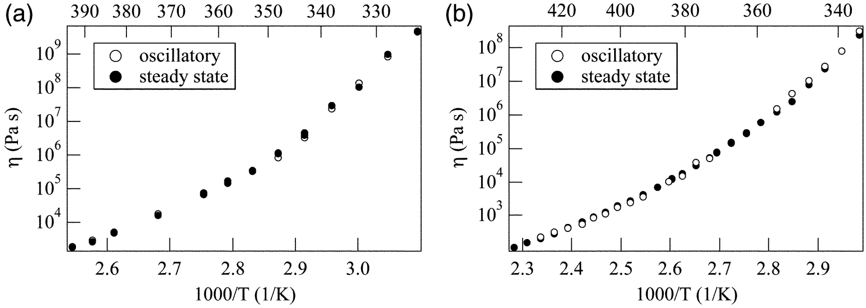

FIGURE 2 Zero shear viscosity for the 30/70 copolymer (a) and the 40/60 copolymer (b). The oscillatory measurements are open symbols and the steady state measurements are bullets.

superimposable (Fig. 2) confirm that TTS also holds for these side group polymers. This is in agreement with previous results on similar side chain liquid crystal polymers [7,8], which showed a failure of TTS only for samples with very high molar masses [7].

According to TTS, the dependence of the shear elastic complex modulus on ω and T can be written as a function of the shear elastic complex modulus measured at the reference temperature T_r [9]:

$$G^*(\omega, T) = b_{T_r}(T)\ G^*(a_{T_r}(T)\omega, T_r). \tag{2}$$

The vertical and horizontal shift parameters, $b_{T_r}(T)$ and $a_{T_r}(T)$, are two real temperature-dependent functions. The $a_{T_r}(T)$ factor strongly depends on temperature and follows the Williams-Landel-Ferry law (WLF) [9]:

$$-\log a_{T_r}(T) = \frac{C_1(T - T_r)}{C_2 + T - T_r}. \tag{3}$$

Master curves and horizontal and vertical shift factors at the reference temperature are obtained by means of a numerical shift of the experimental isothermal frequency sweeps of $G^*(\omega)$ [10].

TABLE 2 VF Eq. (1) Best-Fit Parameters

Copolymer	T_b (K)	T_0 (K)	η_∞ (Pa·s)
PMA4 30/70	1570 ± 30	266 ± 2	$(7.5 \pm 0.3) \cdot 10^{-3}$
PMA4 40/60	1960 ± 50	258 ± 2	$(2.0 \pm 0.2) \cdot 10^{-3}$

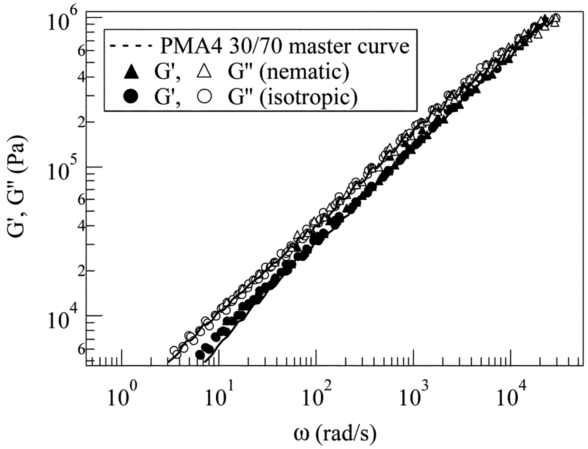

FIGURE 3 Master curves for the 30/70 copolymer at the reference temperature $T_r = 388\,\mathrm{K}$ obtained by shifting data recorded at various temperatures in different phases.

Figure 4 illustrates the master curves of the two copolymers with reference temperatures at the almost isofrictional regime with the same C_1 ($T_r = 388\,\mathrm{K}$ and $T_r = 407\,\mathrm{K}$ for the 30/70 and 40/60 copolymers, respectively). In both master curves, a liquid behavior is observed in the low frequency side. Both copolymers show quite parallel loss

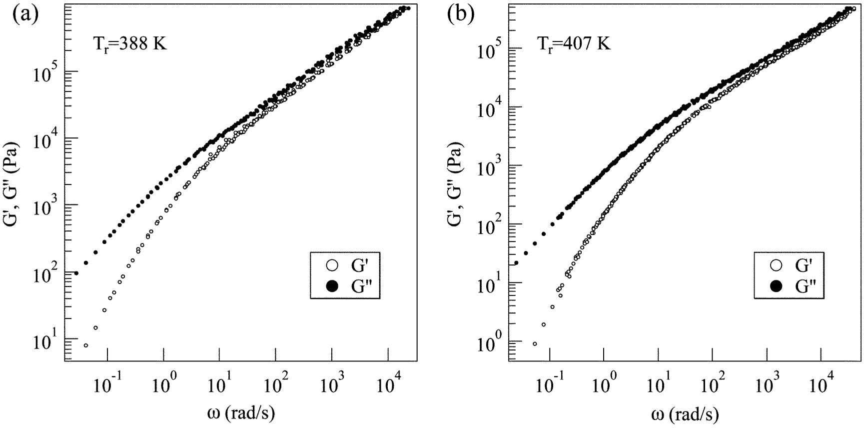

FIGURE 4 Master curves of storage (empty circles) and loss moduli (filled circles) for the 30/70 copolymer at $T_r = 388\,\mathrm{K}$ (a) and 40/60 copolymer at $T_r = 407\,\mathrm{K}$ (b).

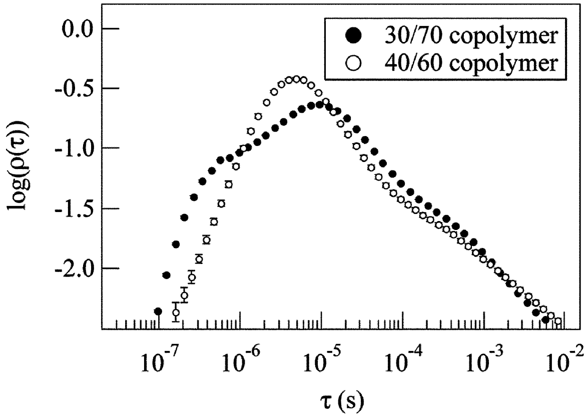

FIGURE 5 Relaxation time distribution $\rho(\tau)$ for the 30/70 copolymer and the 40/60 copolymer.

and storage modulus master curves over a wide frequency range, following the power law $G', G'' \sim \omega$. This behavior is expected in the modified Rouse theory for undiluted polymers and is a known property for polymers with molar masses near the minimum values for entanglement coupling in the region between the terminal zone and the glassy zone [9]. In various acrylic polymers such a rubbery plateau, characteristic of the entangled dynamics, first appears roughly at the critical molar mass $M'_c \sim 3\, M_e \sim 150$ Kuhn segments [11], with M_e the entanglement mass. However, the absence of entanglement was also inferred from the master curves of several azobenzene polymethacrylates [8], even at molar masses expected to be above M'_c. The lack of such a plateau in these side group nematic polymers could be ascribed to the mesophase order that dilates the confining tube, on which dimension the M_e value depends [11], and shifts entanglement to higher molar masses.

The relaxation time distribution $\rho(\tau, T_r)$ was calculated with a nonlinear regularization method [12] from the master curves of PMA4 30/70 and 40/60. The curves $\rho(\tau, T_r)$ of the relaxation time distributions for the 30/70 and the 40/60 copolymers calculated at T_r are shown in Figure 5.

The WLF parameters C_1 and C_2 at T_r were obtained by fitting $a_{T_r}(T)$ for the 30/70 and 40/60 copolymers with Eq. (3) (Table 3). Adopting the Doolittle equation within the TTS framework, one can write $T_0 = T_r - C_2$ and $T_b = C_1 C_2 \cdot \ln 10$, that express the VF parameters as a function of the WLF ones [9]. The fit parameters for the

TABLE 3 WLF Eq. (3) Best-Fit Parameters at T_r and Temperature Invariants

Copolymer	C_1	C_2 (K)	T_r (K)	$C_1\,C_2 \cdot \ln 10$ (K)	$T_r - C_2$ (K)	C_1^g	C_2^g (K)
PMA4 30/70	5.7	122	388	1600	266	14	48
PMA4 40/60	5.9	149	407	2000	258	14	62

30/70 and 40/60 copolymers confirmed the validity of these relations within the experimental error (Tables 2 and 3). This provides further evidence that the rheological properties of these copolymers are dominated by the polymer backbone [7]. Furthermore, being C_1C_2 and $T_r - C_2$ constants independent of T_r, any further dependence on polymer chain mobility can be removed in C_1 and C_2 by extrapolating the WLF parameters C_1^g and C_2^g at T_g [11] (Table 3).

We now consider the fragility of the PMA4 copolymers. Various methods have been suggested in literature to evaluate the fragility of a polymer, that characterizes the way by which the temperature modifies the properties of a given material [13]. The relaxation mechanisms of fragile polymers follow a VF behavior, while strong polymers tend to follow an Arrhenius dependence. Thus, when writing the VF law as

$$\eta = \eta_\infty \exp\left(\frac{DT_0}{T - T_0}\right), \tag{4}$$

the $D = T_b/T_0$ parameter is often used to indicate the fragility of a polymer [13]. The greater D is, the stronger the polymer is. If D tends to infinity, Eq. (4) becomes an Arrhenius-like activated process.

Another way to evaluate the fragility of a polymer is to plot viscosities in a rescaled Angell plot [14] where the rescaled viscosity

$$\log\left[\frac{\eta(T)}{\eta(T_g)}\right] \Big/ \log\left[\frac{\eta(T_g)}{\eta(\infty)}\right] \tag{5}$$

is plotted vs. T_g/T. From such a plot, one can examine how the relaxation mechanisms of the polymer tent to their asymptotic behavior. In particular, according to the Doolittle equation [9], this plot represents the temperature dependence of the free volume ratio function $f(T_g)/f(T) - 1$, and its curvature (fragility) is sensitive to the ratio $T_g/(T_g - T_0)$.

The dynamic fragility is instead a more local definition

$$m = \left.\frac{d\log\tau}{d(T_g/T)}\right|_{T=T_g} = \frac{1}{\ln 10}\frac{T_bT_g}{(T_g - T_0)^2} = T_g\frac{C_1^g}{C_2^g}. \tag{6}$$

m is also referred to as *steepness index* [15]. As it accounts for the slope of the dynamic behavior of relaxation process only at T_g, not necessarily *a priori* correlations between m, D and $T_g/(T_g - T_0)$ are expected. Moreover, even if often m has been correlated to the thermodynamic steepness index, as defined in terms of the variation of the specific heat at the glass transition $\Delta C_p(T_g)$, no clear connections between thermodynamic and dynamic steepness index have been found yet [16].

The rescaled Angell plots for PMMA homopolymer [17], PMA4 homopolymer, and 30/70 and 40/60 copolymers are shown in Figure 6. The fragility parameters D and $T_g/(T_g - T_0)$, and the dynamic fragility m for these samples are reported in Table 4. They follow the same trends from the strongest PMMA sample to the most fragile PMA4 homopolymer (Table 4 and Fig. 6). In this behavior, the influence of the molar mass on the fragility can be confidently ruled out, the four samples having comparable molar masses. In addition, they all possess a polymethacrylate chain and only differ for the relative

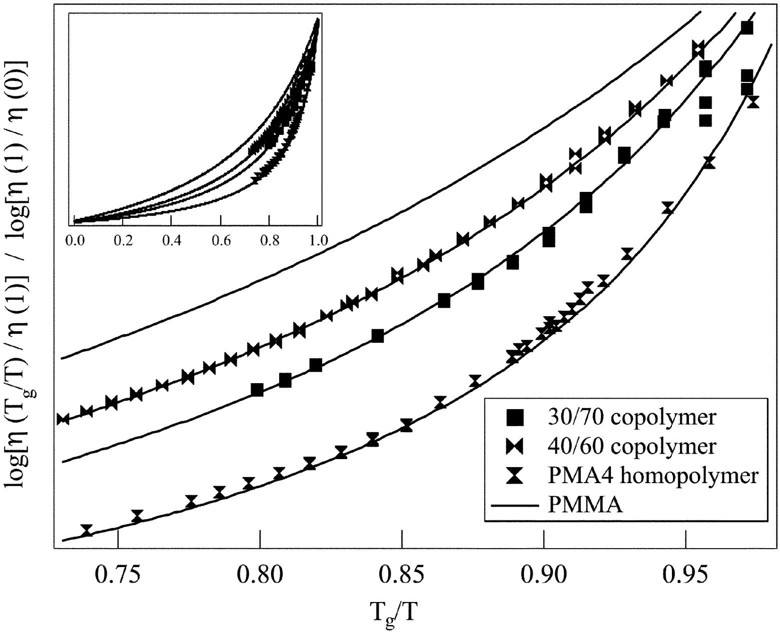

FIGURE 6 Rescaled Angell plot Eq. (5) for PMMA [17] and PMA4 homopolymers and copolymers. The inset contains the traces of the viscosity calculated over the overall accessible temperature range.

TABLE 4 Glass Transition Temperature T_g, Strength Parameters $D = T_b/T_0$ and $T_g/(T_g - T_0)$, and Dynamic Fragility m for PMMA and PMA4 Homopolymers and the 30/70 and 40/60 Copolymers

	PMMA [17]	PMA4 40/60	PMA4 30/70	PMA4 [5]
D	14.3	7.6	5.9	4.0
$T_g/(T_g–T_0)$ (K)	3.8	5.2	6.5	11.3
m	56	72	92	190
T_g (K)	390	320	314	305

contents of more or less bulky side groups. Therefore, the observed trend of the fragility is in agreement with the one expected in going from more to less symmetric main chain structure [18], as determined by incorporation of the side groups in copolymers. Moreover the side chains also affect the rigidity of the polymer main chain as revealed by the values of the glass transition temperature, that increase from fragile PMA4 to strong PMMA. A correlation can be then inferred between the enhanced rigidity of the polymer chain and the stronger character of the system [19].

CONCLUSIONS

We studied the rheological behavior of different PMA4 copolymers in the linear response regime for which the time-temperature superposition principle holds in the overall range of temperature. WLF invariants were also obtained and provide further evidence that the rheological properties of these copolymers are dominated by the structure of their backbone. However, the effects of the side groups were recognized in the absence of the entanglement regime at the molar masses under investigation. An increasing trend was also observed for the fragility of the polymers in the sequence PMMA homopolymer, PMA4 40/60, PMA4 30/70, PMA4 homopolymer, which was also connected with the symmetry of the polymer architecture and the rigidity of the polymer main chain.

REFERENCES

[1] (a) Yaroshchuk, O., Bidna, T., Dumont, M., & Lindau, J. (2004). *Mol. Cryst. Liq. Cryst.*, *409*, 229.
(b) Residori, S. & Petrossian, A. (2003). *Mol. Cryst. Liq. Cryst.*, *398*, 137.
(c) Nakano, M., Yu, Y., Shishido, A., Tsutsumi, O., Kanazawa, A., Shiono, T., & Ikeda, T. (2003). *Mol. Cryst. Liq. Cryst.*, *398*, 1.
(d) Meier, J. G., Ruhmann, R., & Stumpe, J. (2000). *Macromolecules*, *33*, 843.

(e) Bubliz, D., Helgert, M., Fleck, B., Wenke, L., Hvilsted, S., & Ramanujam, P. S. (2000). *Appl. Phys. B*, *70*, 803.

[2] Andreozzi, L., Faetti, M., Galli, G., Giordano, M., & Palazzuoli, D. (2004). *Macromol. Symp.*, *218*, 323.

[3] Andreozzi, L., Faetti, M., Galli, G., Giordano, M., & Palazzuoli, D. (2001). *Macromolecules*, *34*, 7325.

[4] Likodimos, V., Labardi, M., Pardi, L., Allegrini, M., Giordano, M., Arena, A., & Patanè, S. (2003). *Appl. Phys. Lett.*, *82*, 3313.

[5] Andreozzi, L., Faetti, M., Giordano, M., Zulli, F., Galli, G., & Laus, M. (2005). *Mol. Cryst. Liq. Cryst.*, *429*, 301.

[6] Angeloni, A. S., Caretti, D., Laus, M., Chiellini, E., & Galli, G. (1991). *J. Polym. Sci., Polym. Chem. Ed.*, *29*, 1865.

[7] Berghausen, J., Fuchs, J., & Richtering, W. (1997). *Macromolecules*, *30*, 7574.

[8] Colby, R. H., Gillmor, J. R., Galli, G., Laus, M., Ober, C. K., & Hall, E. (1993). *Liq. Cryst.*, *13*, 233.

[9] Ferry, J. D. (1980). *Viscoelastic Properties of Polymers*, Wiley: New York.

[10] Honerkamp, J. & Weese, J. (1993). *Rheol. Acta.*, *32*, 57.

[11] Fetters, L. J., Lohse, D. J., Richter, D., Witten, T. A., & Zirkel, A. (1994). *Macromolecules*, *27*, 4639.

[12] (a) Honerkamp, J. & Weese, J. (1993). *Rheol. Acta.*, *32*, 65.
(b) Weese, J. (1993). *J. Comput. Phys. Commun.*, *77*, 429.

[13] Angell, C. A. (1984). In: *Relaxation in Complex Systems*, Ngai, K. & Wright, B. G. (Eds.), National Technical Information Service, U.S. Department of Commerce: Springfield, VA, 203.

[14] Angell, C. A. (1997). *J. Res. Nat. Inst. Stand. Technol.*, *102*, 171.

[15] Plazek, D. & Ngai, L. K. (1991). *Macromolecules*, *24*, 1222.

[16] (a) Huang, D. & McKenna, G. B. (2001). *J. Chem. Phys.*, *114*, 5621.
(b) Andreozzi, L., Faetti, M., Giordano, M., & Palazzuoli, D. (2003). *J. Phys. C: Cond. Matt.*, *15*, S1215.

[17] Fuchs, K., Friedrich, C., & Weese, J. (1996). *Macromolecules*, *29*, 5893.

[18] Ngai, L. K. & Roland, M. (1993). *Macromolecules*, *26*, 6824.

[19] Ding, Y., Novikov, V. N., Sokolov, A. P., Cailliaux, A., Dalle-Ferrier, C., Alba-Simionesco, C., & Frick, B. (2004). *Macromolecules*, *37*, 9264.